THE INFLUENCE OF TEMPERATURE AND CHLORIDE/SULPHATE CONCENTRATION ON THE PASSIVE BEHAVIOUR OF GRADE-7 TITANIUM

D. Ofori, J.J. Noël, D.W. Shoesmith
Undergrad
Department of Chemistry,
The University *of* Western Ontario,
London, Onatrio, Canada, N6A 5B8

Abstract

Titanium is protected against corrosion by a thin surface oxide film which may be only a few nanometers thick, and the chemical and physical durability of this film must be maintained if this metal and its alloys are to be used in industrial applications. Previous studies suggest that a temporary loss of passivity under high temperature aqueous conditions occurs at the grain boundaries in the material. The frequent breakdown and repair of the film yields electrochemical signals in the form of potential transients in the corrosion potential. The analysis of these potential signals provides very valuable information concerning the electrochemical behaviour of the alloy under these conditions.

In this study, the electrochemical signals generated on Titanium (grade 7) were measured in aqueous chloride and sulphate solutions as a function of temperature (up to 150°C). In one experiment, the Ti-7 sample was allowed to form an air oxide film prior to exposure to the solution. Electrochemical impedance spectroscopy (EIS) was used to characterize the electrical properties of the film in each of the scenarios described above. By fitting EIS results to equivalent electrical circuits the consequences of film breakdown and repair on the overall film resistance were determined.

Introduction

Titanium is the ninth most abundant element on the planet and the fourth most abundant metal [1]. It has two elemental crystal structures, namely alpha and beta. In the beta (β) phase, the atoms are arranged in a body-centered cubic (BCC) array, where as in the alpha (α) phase they are arranged in a close-packed hexagonal (HCP) array [1]. The BCC arrangement of the atoms is only found at high temperatures unless titanium is alloyed with other elements to maintain the cubic structure at low temperatures. In such alloys, regions of beta phase are located along the alpha grain boundaries. Unalloyed α-titanium, referred to as commercially pure (CP), has a very good corrosion resistance. Pure titanium can be strengthened or its corrosion resistance improved by alloying with various elements which can dissolve as a mixture in titanium substituting for titanium atoms. Alloying elements are generally classified as neutral, α-stabilizers or β-stabilizers. For example, Al which is an α-stabilizer, increases the temperature at which the α-phase is stable. Other examples of α-stabilizers include O, N, and C. Elements such as Fe, V, Mo, Mn, result in stability of the β-phase at lower temperatures [1] and therefore are known as β-stabilizers.

There is a limit in terms of solubility for alloying and impurity elements in titanium. Thus, when the impurity Fe is present in excess of its solubility it tends to precipitate to form intermetallic compounds such as Ti_xFe. To counteract the effect of Fe impurity, Pd is added in varying amounts, depending on the application, to increase the corrosion resistance. Grade-7 titanium contains ~0.2%wt of the alloying element Pd. Pd acts as an α-stabilizer and therefore dissolves throughout the α-phase thereby preventing the separation of the β-phase.

Commercially pure titanium and the alpha and near-alpha titanium alloys generally demonstrate the best general corrosion-resistance qualities among the family of titanium alloys. It is for this reason that titanium grade 7 was selected by the U.S. Department of Energy as the material for the fabrication of drip shields in the proposed nuclear waste repository at Yucca Mountain [2,3]. The focus of this project is to determine how the passive state (a state of low corrosion rate, even under high anodic driving force) of titanium grade 7 is influenced by temperature in solutions containing the aggressive chloride and the sulphate anions, both of which are expected to be present in groundwater contacting the drip shield.

Experimental

- *Electrochemical Cell and Electrodes*

A schematic of the electrochemical cell used is shown in fig 1. The cell was built within a titanium pressure vessel (Parr Instrument Co., model 4621). The pressure vessel and lid were made of ASTM Grade-4 titanium. The lid was modified to accept four sealing glands for electrode feed-throughs. The working electrode was positioned near the centre of the cell and was suspended in solution by a titanium welding rod sheathed in 4 mm diameter heat-shrink Teflon tubing. Approximately three-quarters of the electrode surface was immersed into solution. The counter electrode, having the same composition as the titanium metal was modified into a cylindrical shape to enclose the working electrode. The working electrode was galvanically coupled to the counter electrode through a zero resistance ammeter (Keithley, model 6514). A homemade internal Ag/AgCl (0.1M KCl) reference electrode was used to monitor the open circuit potential (E_{corr}) of the working electrode. All potentials are quoted against this reference electrode at the specific temperature employed. The electrochemical cell was lined with a solid teflon liner in order to avoid direct solution contact with the pressure vessel walls.

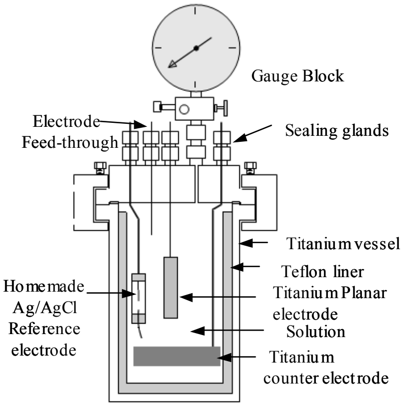

Fig 1. The electrochemical cell

To prevent boiling of the electrolyte solution upon heating, the pressure vessel was pressurized with 60 psi of UHP Argon gas. The experimental temperature was controlled by an autoclave heater (Parr Instrument Co. model 4913) and measured using a thermocouple. Rectangular-shaped working electrodes of dimensions 20 mm × 5 mm × 5 mm were cut from titanium plates. A 3mm centered hole was drilled into each planar electrode at one end. This enabled the electrode to accept the threaded titanium rod for suspension within the cell and also to provide electrical contacts to external equipment. Each electrode was manually polished with wet silicon carbide papers in the order of 120, 220, 320, 500 then 600 grit levels. Each electrode was then rinsed by sonication in a methanol/deionized water mixture.

- *Experimental Procedure*

All experiments were conducted in 0.1 M NaCl and 0.1 M Na_2SO_4 solutions. For each experiment the solution was aerated by vigorous agitation in air. Fig 2 illustrates the sequence of electrochemical measurements employed during each experiment. The corrosion potential (E_{corr}) of the working electrode was measured against the Ag/AgCl (0.1 M KCl) reference electrode for approximately 22 hours to achieve a steady state condition. An EIS measurement was then made by coupling the working electrode and the Ag/AgCl reference electrode with a titanium counter electrode in a circuit controlled by a potentiostat (Solartron model 1287) coupled to a frequency response analyzer (FRA, Solartron model 1255B). The applied potential was varied sinusoidally at a series of single frequencies over the range of 10^5 to 10^{-3} Hz, with the FRA integration time set to 0.2 seconds, using a voltage amplitude of ± 10 mV. The measured EIS spectra were least-squares fitted to equivalent circuits using ZView for Windows software (version 2.3d, Scribner Associates Inc.).

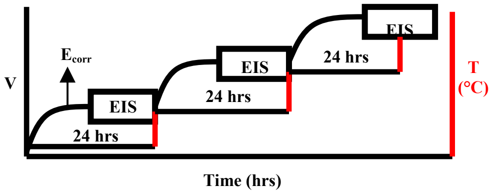

Fig 2. General experimental procedure employed as a function of time & temperature

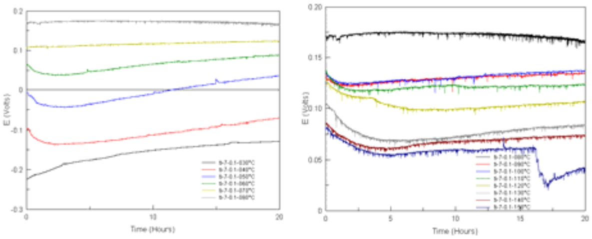

Fig 3. E_{corr} measured on Ti-7 in 0.1M NaCl at elevated temperatures

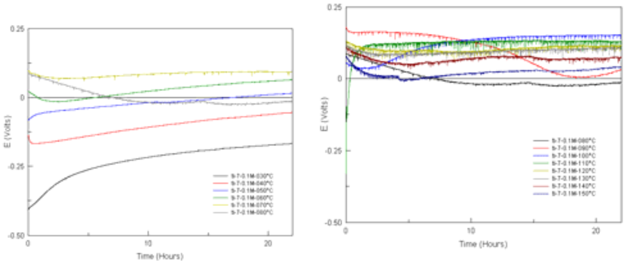

Fig 4. E_{corr} measured on Ti-7 in NaCl at elevated temperatures using an electrode with an air-formed oxide

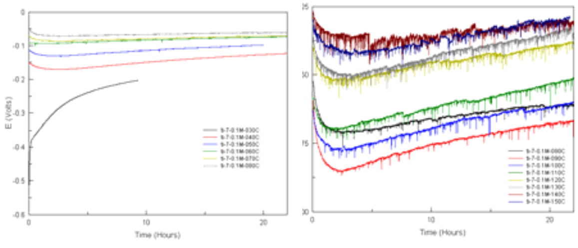

Fig 5. E_{corr} measured on Ti-7 in 0.1M Na_2SO_4 at elevated temperatures

Results and Discussion

- *Comparison of Behaviour of Ti-7 as a function of Chloride and Sulphate solution*

Figs 3, 4 & 5 show the E_{corr} results recorded on Ti-7 at elevated temperatures in 0.1 M NaCl and 0.1 M Na_2SO_4 solutions. In these experiments, the temperature was raised daily from 30°C to 150°C in 10°C increments. After measuring E_{corr} for approximately 22 hours an EIS was measured at each temperature. The temperature was then increased and the procedure repeated.

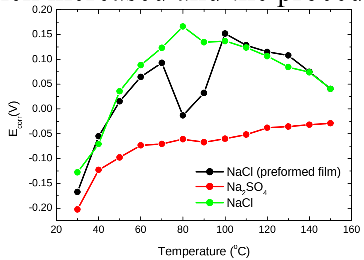

Fig 6. E_{corr} as a function of temperature for Ti-7 in 0.1M NaCl and 0.1M Na_2SO_4

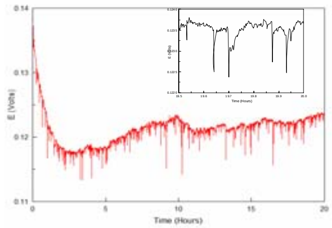

Fig 7. Expanded section of the E_{corr}-time plot recorded on Ti-7 in 0.1M NaCl at 110°C

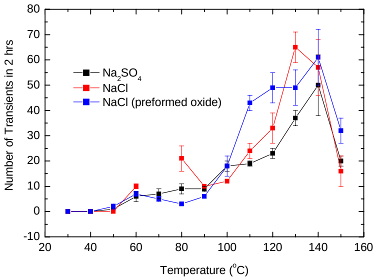

Fig 8. E_{corr} transient activity in 2hrs period for Ti-7

Shown in fig 6 are the E_{corr} values for the experiments conducted in the chloride and sulphate solutions. In the chloride solution, there is an initial rise in E_{corr} with temperature (up to ~ 80°C) followed by an eventual decrease at higher temperatures ($T > 80°C$). The behaviour observed in the sulphate solution is different. E_{corr} does not increase to the same extent as observed for the chloride solution for $T \leq 80°C$, and it does not decrease at temperatures > 80°C. However, a very significant feature is the onset of noise signals superimposed on the E_{corr} measurement in the temperature range within which E_{corr} changes direction from increasing with temperature to decreasing with temperature; i.e. T~ 80°C. These noise signals were in the form of negative-going potential transients. Fig 7 shows an expanded section of the E_{corr}-time plot recorded on Ti-7 in 0.1 M NaCl at 110°C. A closer inspection of these transients shows that they have a sharp leading edge followed by a slower exponential recovery period. The recovery however is often quite uneven.

The rapid initial decrease in E_{corr} is indicative of a local film fracture event and the exponential increase in E_{corr} back to the original value prior to the event indicates that the fracture repairs via a film re-growth process. The time required for the potential transient to return to its original value is a measure of the repassivation time. However, since only a potential is measured, no direct kinetic information is obtained.

An analysis of the transient activity yields a plot of the number of transients in a 2-hour period as a function of temperature for both chloride and sulphate solutions as shown in fig 8. In both chloride and sulphate solutions, the generation of signals begins around 60°C, but becomes significant around 80°C and then increases steadily with temperature. This observation is consistent with the results of previous investigations [2, 4]. Up to ~100°C, the signal frequency is very similar in both solutions. However, the frequency of events is greater for chloride than it is for sulphate over the temperature range 100°C to 140°C. Finally, for both solutions there is a very significant decrease in signal frequency at a temperature of 150°C. This may mean that the number of available fracture sites is limited and they have all been utilized by the time 150°C is reached.

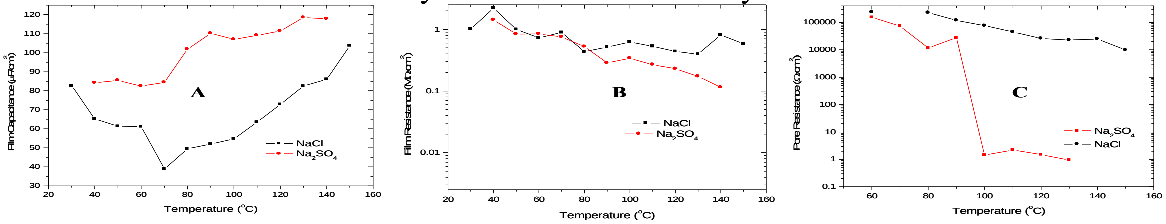

Fig. 9 Comparison of A) film capacitance, B) film resistance, and C) pore resistance values for Ti – 7 in 0.1 M NaCl and 0.1 M Na_2SO_4 solutions determined by fitting of experimental EIS data

An analysis of the impedance properties of the film was performed by EIS. The spectra can be fitted using equivalent electrical circuits that simulate the impedance properties of the passive interface. From these plots values for the resistance and capacitance of the film can be obtained. In this case the data was found to fit to a two time constant circuit representing an oxide film containing pores or flaws.

Fig 9A shows the plot of film capacitance as a function of temperature for the chloride and sulphate solutions. The trends observed are as follows:

- At low temperatures ($T < 80°C$), the capacitance data obtained in chloride solutions show a decrease as the potential increases. This behaviour can be attributed to either (or both) film thickening or the annealing of defects with temperature. The data obtained in sulphate solution, however, show no change in capacitance at low temperatures. This suggests that either the film properties do not change with temperature, or that film thickening (which would involve a decrease in capacitance) and an increase in number of defects (which would involve an increase in capacitance) counteract each other.

- At high temperatures (T ≥ 80°C), the capacitance of the film increases in both solutions. This could be interpreted as due to a decrease in film thickness or to an increase in number of defects in the film. The probability of the film thinning is ruled out because the protective oxide film on titanium is virtually insoluble. Therefore, the increase in film capacitance is most likely due to introduction of flaws due to the observed film fracture events. The most likely explanation for the increase in capacitance is the incorporation of water into repaired fracture sites which would lead to a substantial increase in the effective dielectric constant of the film.

Fig 9B shows a plot of film resistance plotted against temperature for the chloride and sulphate solutions. It was observed that the film formed in both solutions exhibits similar resistive behaviour at low temperatures with only a slight decrease in film resistance being observed. However, at temperatures above 80°C, the film resistance obtained in a chloride solution is significantly greater than that obtained in a sulphate solution. The film resistance in chloride solution is maintained approximately constant for temperatures above 80°C whereas that of the sulphate decreases steadily with temperature.

Fig 9C shows a plot of the pore resistance as a function of temperature. This plot reveals a significant difference in behaviour between the two solutions. At low temperatures, the chloride and the sulphate pore resistances are similar. However, at high temperatures, the pore resistance in sulphate is effectively zero whereas that in the chloride remains > 10^4 Ω.

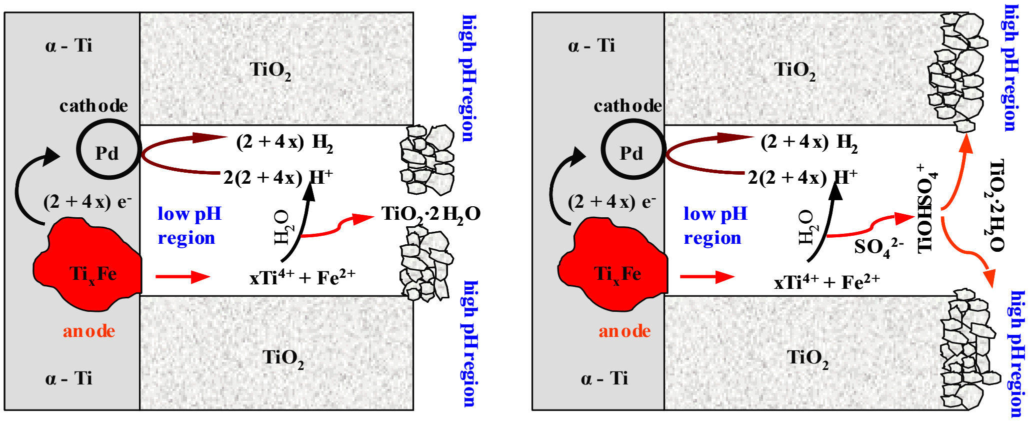

Fig. 10 Schematic illustration of the corrosion and repassivation processes occurring in a sub-micron size fracture site in the oxide film on Ti-7 in 0.1 M NaCl and 0.1M Na_2SO_4 solution

Fig 10 schematically illustrates the mechanism by which corrosion and repassivation occurs within fracture sites in the original passive oxide. When a flaw is introduced into the oxide film via film fracture, the bare titanium surface is exposed to solution. When the metal is exposed, the dissolution of the intermetallic located at the β-phase occurs, producing Ti^{4+} which then hydrolyzes in water to produce protons, leading to acidification of the site. If the acidity remains trapped within the site then the rate of dissolution of the intermetallic to produce Ti^{4+} will remain high and corrosion will continue. The coupling of an anodic reaction to a cathodic reaction is the fundamental basis of general corrosion. Therefore the corrosion of titanium involves the coupling of the Ti_xFe anodic dissolution to proton reduction; i.e.

$$\mathbf{Ti_xFe \rightarrow x\,Ti^{4+} + Fe^{2+} + (2 + 4x)\,e^-} \qquad \mathbf{(1)}$$

$$\mathbf{2(2 + 4x)\,H^+ + 2(2 + 4x)\,e^- \rightarrow (2 + 4x)\,H_2} \qquad \mathbf{(2)}$$

However, for a shallow site, H^+ can diffuse down the concentration gradient and out of the fracture site into the bulk solution. This will prevent extreme acidification. The increase of the pH in the fracture site will decrease the rate of titanium dissolution and allow the formation of an oxide film at the surface of the bare titanium. Hence, repassivation of the bare metal will occur

$$\mathbf{Ti + 2H_2O \rightarrow TiO_2 + 4H^+} \qquad \mathbf{(3)}$$

Pd is well known as a catalyst for proton reduction. Hence, the Pd added during the fabrication of grade-7 titanium, which is distributed throughout the matrix of the α-phase, accelerates reduction of the protons, thereby decreasing the acidity at the fracture site. The increase in pH allows the formation of TiO_2 (equation 3) to occur rapidly. A rapid repassivation process via film regrowth will lead to a rapid exponential rise in potential back to the initial value before the decease.

At the high temperatures employed in this work, anodic dissolution of Ti_xFe intermetallics leads a substantial dissolved Ti^{4+} concentration in the fracture site. During the period of fracture and repassivation, some Ti^{4+} diffuses out of the low pH region to a region of high pH (pH=7) where it precipitates forming $TiO_2{\cdot}2H_2O$. The precipitation of $TiO_2{\cdot}2H_2O$ in the chloride solution appears to occur within the fracture/flaw leading to a high pore resistance.

The mechanism by which the $TiO_2{\cdot}2H_2O$ crystallites are formed in the sulphate solution is similar to that described above for chloride. However, the difference between the two solutions is that the amount of Ti^{4+} diffusion is greater in sulphate compared to that of the chloride, since sulphate has the ability to complex with Ti^{4+} forming $TiOHSO_4^+$. Therefore the solubility is higher due to the additional complexation. The titanium-sulphate complex can then escape the fracture site before depositing as $TiO_2{\cdot}2H_2O$ outside of the pore. This leads to a negligible pore resistance in the sulphate solution. Despite this difference, the overall film resistance, fig 9C, remains high in both solutions. This confirms that the oxide growth reaction via equation 2 is a major contributor to the overall passivity of titanium grade-7.

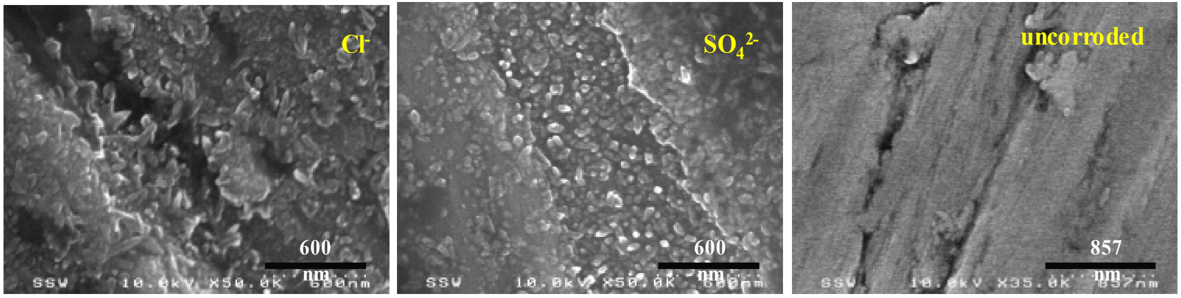

A B C

Fig. 11 SEM images of Ti-7 after exposure to 0.1 M NaCl (A), 0.1 M Na_2SO_4 (B), and the uncorroded surface (C)

Fig 11 shows the SEM images of the uncorroded surface and the surfaces after exposure to the chloride and sulphate solutions. Corrosion in both chloride and sulphate leads to the accumulation of small crystallites roughly 50 to 100 nm in size. The number of such crystallites appears greater after exposure to sulphate than to chloride solution. The chemical composition of these crystallites has not been analyzed, but is most certainly a hydrated titanium dioxide ($TiO_2 \cdot 2H_2O$). The presence of these crystallites confirms the claim that titanium dissolution occurs within the fracture sites before repassivation occurs.

Summary and Conclusion

- The onset of oxide film fracturing on Ti-7 commences around ~ 80°C in both chloride and sulphate solutions.
- The frequency of breakdown events is greater in chloride solutions that in sulphate solutions for $T > 100°C$.
- In both solutions the fracture sites repassivate. This can be attributed to the catalytic effect of the Pd in the alloy which catalyzes proton reduction thereby preventing the development of very acidic conditions. This allows the site to repassivate.
- Due to the ability of SO_4^{2-} to complex Ti^{4+} more corrosion damage occurs in sulphate solutions compared to chloride solutions. This is indicated by the lower polarization and pore resistances obtained in sulphate solutions.
- Repassivation in chloride solution involves precipitation of $TiO_2 \cdot 2H_2O$ in the fracture site. In sulphate solution precipitation occurs outside the site.

Acknowledgements

This research is funded by the Canadian Natural Sciences and Engineering Research Council (NSERC). we also would like to thank Pellumb Jakupi for his help with the experimental setup and Surface Science Western for their help with SEM.

Reference

1. Mathew J. Donachie Jr. Titanium: A Technical Guide. 2nd Edition. Materials Park, OHIO: ASM International, 2000.
2. X. He. Effects of Temperature, Impurities (Fe), and Alloy Elements (Ni, Mo, Pd) on the Crevice Corrosion of Alpha Titanium Alloys. Ph. D Thesis, The University of Western Ontario, 2003.
3. G. M. Gordon. Corrosion considerations related to permanent disposal of high-level radioactive waste. Corrosion 58 (2002), 811-825
4. P. Jakupi. Analysis of Potential Signals from Passive Titanium Alloy Electrodes. BSc. (honors) thesis, The University of Western of Ontario, 2004.